Journal of ELECTRONIC MATERIALS, Vol. 40, No. 2, 2011
DOI: 10.1007/s11664-010-1447-2
© 2010 TMS

Interdependent Intermetallic Compound Growth in an Electroless Ni-P/Sn-3.5Ag Reaction Couple

ADITYA KUMAR[1] and ZHONG CHEN[1,2]

1.—School of Materials Science and Engineering, Nanyang Technological University, 50 Nanyang Avenue, Singapore 639798, Singapore. 2.—e-mail: ASZChen@ntu.edu.sg

The interfacial microstructure of electroless Ni-P/Sn-3.5Ag solder joints was investigated after reflow and high-temperature solid-state aging to understand its interdependent growth mechanism and related kinetics of intermetallic compounds (IMCs) at the interface. The reflow and aging results showed that mainly three IMC layers, Ni_3Sn_4, Ni_2SnP, and Ni_3P, formed during the soldering reaction. It was found that the Ni_3Sn_4 and Ni_3P layers grow predominantly as long as the electroless Ni-P layer is present; however, once the Ni-P layer is fully consumed, the Ni_2SnP layer grows rapidly at the expense of the Ni_3P layer. A transition in the Ni_3Sn_4 morphology from needle and chunky shape to scallop shape was observed after the solid-state aging of reflowed samples. The kinetics data obtained from the growth of compound layers in the aged samples revealed that initially the growth of the Ni_2SnP layer is controlled by diffusion, and subsequently by the rate of reaction after the Ni-P metallization is fully consumed. It was found that complete transformation of the electroless Ni-P layer into a Ni_3P layer results in the rapid growth of the Ni_2SnP layer due to the dominating reaction of Sn with Ni_3P. The apparent activation energies for the growth of Ni_3Sn_4, Ni_2SnP, and Ni_3P compound layers were found to be 98.9 kJ/mol, 42.2 kJ/mol, and 94.3 kJ/mol, respectively.

Key words: Electroless Ni-P, intermetallic compound, lead-free solders, kinetics, interfacial reaction, under bump metallization, ENIG

INTRODUCTION

Electroless nickel with a thin layer of immersion gold has been widely used as under bump and substrate metallizations for low-cost solder flip-chip and ball grid array packages.[1,2] Electroless nickel is an amorphous Ni-P alloy (particularly for P > 12.5 at.%).[3] Owing to the presence of P, interfacial reaction between electroless Ni-P and solder is more complicated than for pure Ni, and results in the formation of various intermetallic compounds (IMCs).[1,2,4–22] Solder reaction-assisted crystallization of amorphous electroless Ni-P has been reported in a number of studies.[1,5–8,10] This crystallization leads to the formation of a higher-P-containing Ni-P compound layer in between Ni_3Sn_4 and electroless Ni-P layers. Some researchers have reported that the crystallized electroless Ni-P layer consists of Ni_3P,[1,6] while others report a mixture of Ni_3P and Ni.[5,8,10] In addition to Ni_3P, formation of other Ni-P phases, such as $Ni_{12}P_5$[5] and Ni_2P,[14] has also been reported under extended aging conditions. Leaving these fine details aside, all evidence shows that solder reaction-assisted crystallization of electroless Ni-P under bump metallization leads to formation of a Ni-P compound layer that is dominated by Ni_3P. Furthermore, in a few recent studies, a thin ternary Ni-Sn-P layer has been reported to form in between Ni_3Sn_4 and Ni_3P layers[6–8,10] during liquid-state reaction.[9,14,17] This ternary Ni-Sn-P layer has also been found to grow thicker during solid-state aging, and the underlying Cu can diffuse through this layer to form Cu-Sn intermetallics in the Cu/Ni-P/Sn-3.5Ag solder joint.[18]

(Received March 17, 2010; accepted November 13, 2010; published online December 15, 2010)

The growth of multiple interfacial compounds in the electroless Ni-P/solder system is of great interest, as in several reliability studies, brittle fracture has been found to occur in between these compounds.[7,16,19,20] Although several studies have examined the interfacial reactions between electroless Ni-P and solder,[1,2,4–22] there is little quantitative understanding of how the growth of one IMC layer interacts with its neighboring IMC layers. The reason for this limited understanding is that most of the studies have been carried out either under solid-state aging at low temperatures equal to or below 150°C, or under liquid state at high temperatures above 210°C. At these conditions, interfacial reactions are either too slow or too fast to allow the study of the whole intermediate growth stages. To our knowledge, there has been no report on the growth kinetics of the ternary Ni_2SnP IMC, not to mention how its growth is affected by its neighboring layers. Thus, a thorough investigation is required for intermediate growth conditions that can represent a sufficient window for the observation of all types of IMC layers with the data analyzed interdependently. Accordingly, in this investigation, solid-state aging of electroless Ni-P/Sn-3.5Ag solder joints was carried out at temperatures ranging from 140°C to 200°C for different durations. Particular attention was paid to understanding the growth mechanism and interdependent IMC growth kinetics of different compounds that are formed at the soldering interface.

EXPERIMENTAL PROCEDURES

Cu (99.98 wt.%) plate was used as a substrate for electroless plating of Ni-P metallization for the soldering reaction with lead-free solder Sn-3.5Ag. The Cu plate was first polished by a series of sandpapers down to 1-μm finish, and then ultrasonically cleaned in an acetone bath for 10 min. It was then etched with 20 vol.% HNO_3 solution for a few seconds, and finally rinsed with deionized water. Electroless Ni-P was plated on the surface-cleaned Cu plate in two steps. In the first step, the Cu surface was activated using a ruthenium-based preinitiator. Then, electroless Ni-P was plated on the activated Cu surface. A thin layer ($\sim$0.05 μm) of noncyanide immersion gold was also deposited on the electroless Ni-P surface to protect it from oxidation.

Soldering was carried out using Sn-3.5Ag wire (with flux in core) in an IR reflow oven (ESSEMTEC RO-06E), which involved preheating at 150°C for 100 s, then reflowing at 250°C for 60 s, and finally cooling down to 160°C in the oven. After the reflow, solid-state aging of reaction couples was carried out in an oven (Lenton WHT4/30) at 140°C, 160°C, 180°C, and 200°C for 48 h, 100 h, 225 h, and 400 h. After aging, the samples were removed from the oven and cooled to room temperature in air. A JEOL JSM-6360A scanning electron microscope (SEM) was used for microstructure analysis. For the cross-sectional SEM, the samples were cold-mounted in epoxy and polished down to 1-μm finish. After polishing, solder etching was carried out with 4 vol.% HCl acid for a few seconds to reveal the microstructure. To observe the top view of the interfacial compound, the sample was soaked in 5 vol.% HNO_3 acid for a few minutes to dissolve all the solder. Energy-dispersive x-ray spectroscopy (EDS) was performed in the SEM to analyze the chemical composition of interfacial compounds. Image processing and analysis software was used to measure the area of IMC and length of interfacial compound from the SEM images. The average thickness of the interfacial compound was determined by dividing the area by the length. The measurement was carried out at six different locations in each sample.

RESULTS

Interfacial Microstructure Analysis

SEM and EDS analyses of as-prepared and thermally aged samples were carried out to analyze the formation of interfacial compounds as well as to understand the evolution of the microstructures at the soldering interface.

As-Prepared Sample

The thickness and P content of the as-plated electroless Ni-P layer were measured to be around 9.9 μm and 16 at.%, respectively. Figure 1a and b show cross-sectional and top views of compounds formed at the Sn-3.5Ag/electroless Ni-P interface of the as-prepared sample. It can be seen that needle-shaped and chunky-shaped Ni_3Sn_4 intermetallics formed at the Sn-3.5Ag/electroless Ni-P interface during reflow. Underneath the Ni_3Sn_4 intermetallics, a ternary Ni-Sn-P layer formed, whose composition was difficult to measure by EDS in the SEM owing to its small thickness. However, in our previous study,[10] with the help of transmission electron microscopy, the Ni-Sn-P layer was found to consist of a mixture of Ni_2SnP and Ni. Underneath the Ni-Sn-P layer, a dark, thin Ni_3P layer having a large number of columnar voids was found to form within the electroless Ni-P layer. Formation of these compounds is in agreement with the results of previous interfacial studies between electroless Ni-P and different solders.[1,6,7,9,10] The immersion Au layer that was plated on the electroless Ni-P layer was completely dissolved in the molten solder during reflow, as no Au or Au-Sn intermetallic was found at the Sn-3.5Ag/electroless Ni-P interface.

Thermally Aged Samples

Figure 2 shows back-scattered SEM images showing the growth of various compounds at the Sn-3.5Ag/Ni-P/Cu interfaces in the samples aged at different temperatures. It can be observed that three compound layers, namely Ni_3Sn_4, Ni_2SnP, and Ni_3P,

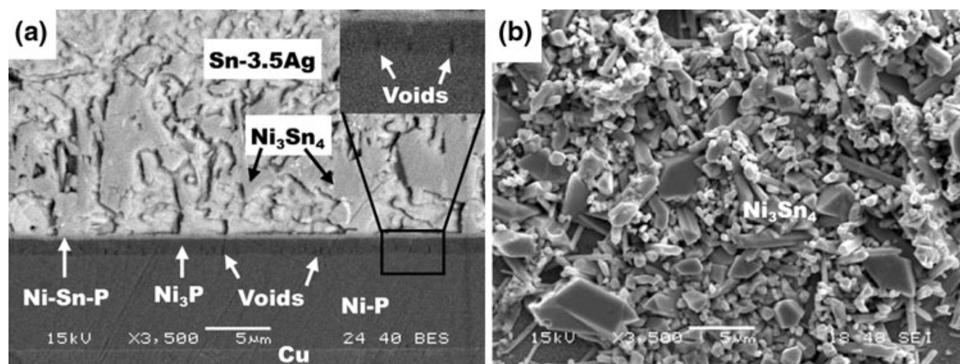

Fig. 1. (a) Cross-sectional and (b) top views of Ni_3Sn_4 formed at the Sn-3.5Ag/Ni-P interface of the as-prepared samples.

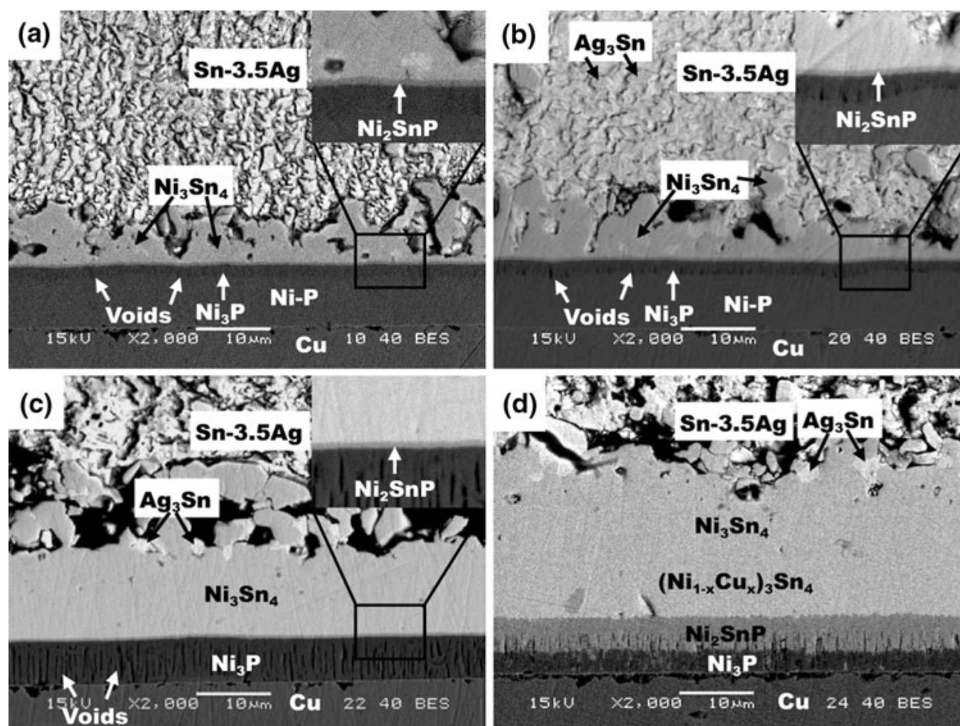

Fig. 2. Back-scattered SEM images showing the growth of Ni_3Sn_4, Ni_2SnP, and Ni_3P compounds at the Sn-3.5Ag/Ni-P/Cu interfaces of the samples aged for 225 h at temperatures of (a) 140°C, (b) 160°C, (c) 180°C, and (d) 200°C.

grew thicker during aging. As the reaction proceeded, columnar voids present in the Ni_3P layer also grew in size as well as in number. The morphology of Ni_3Sn_4 changed into the scallop shape during aging (Fig. 3). In the sample aged at 180°C, most of the electroless Ni-P layer transformed into a Ni_3P layer, as shown in Fig. 2c. The thickness of this transformed electroless Ni-P layer (~5.2 μm) is much smaller than that of the as-plated electroless Ni-P layer (~9.9 μm). The shrinkage indicates that, during aging, Ni diffused out from the electroless Ni-P ($Ni_{84}P_{16}$) layer to form Ni_3Sn_4, leaving behind a higher-P-containing Ni-P (Ni_3P) layer.

In the samples aged at 180°C and 200°C, the Sn-3.5Ag/Ni_3Sn_4 interface became flatter (Figs. 2c, d and 3c, d) and some Ag_3Sn particles accumulated at the interface (Fig. 2c and d) as the Ni_3Sn_4 compound layer expanded. Relatively fast growth of the ternary Ni-Sn-P compound layer and the presence of a small amount of Cu (up to 5 at.%) in the Ni_3Sn_4 compound were observed in samples aged at 200°C (Fig. 2d). The elemental composition of this Ni-Sn-P layer was found to be similar to that of Ni_2SnP. Thus, this layer will be referred to as the Ni_2SnP layer hereinafter.

Figure 4 shows line-scan images of the Cu/electroless Ni-P/Sn-3.5Ag interfaces of samples aged at 200°C for different durations. It is clear that, in the samples aged at 200°C, the original amorphous Ni-P layer completely transformed into a crystalline Ni_3P layer within 48 h of aging, and then the Ni_2Sn-P layer started growing at the expense of

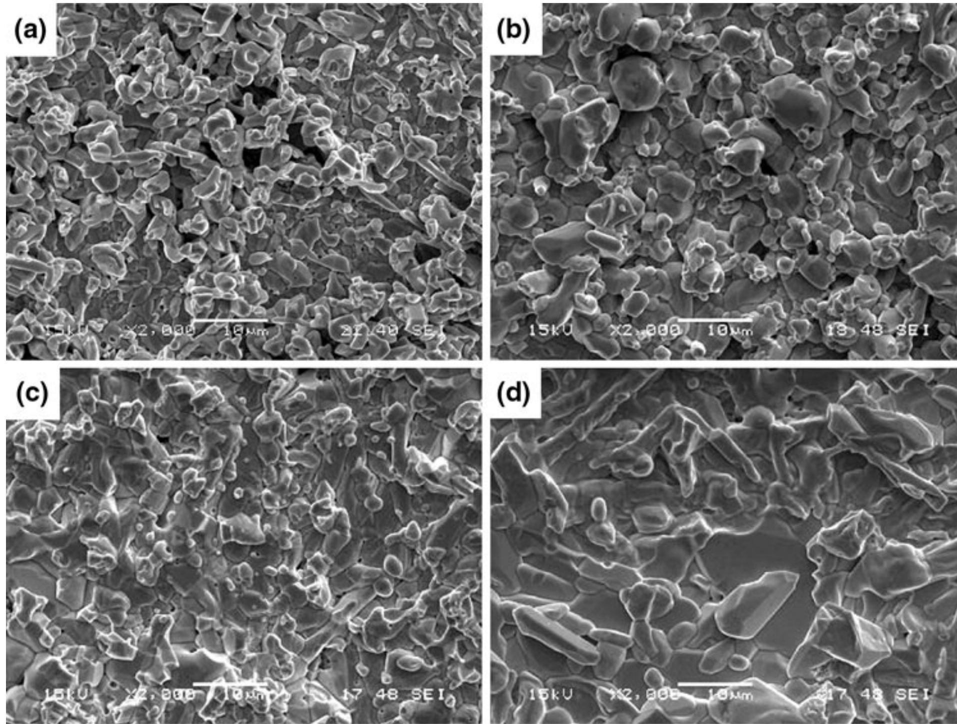

Fig. 3. Top view of Ni_3Sn_4 IMC in the samples aged for 225 h at temperatures of (a) 140°C, (b) 160°C, (c) 180°C, and (d) 200°C, showing scallop-shaped morphology.

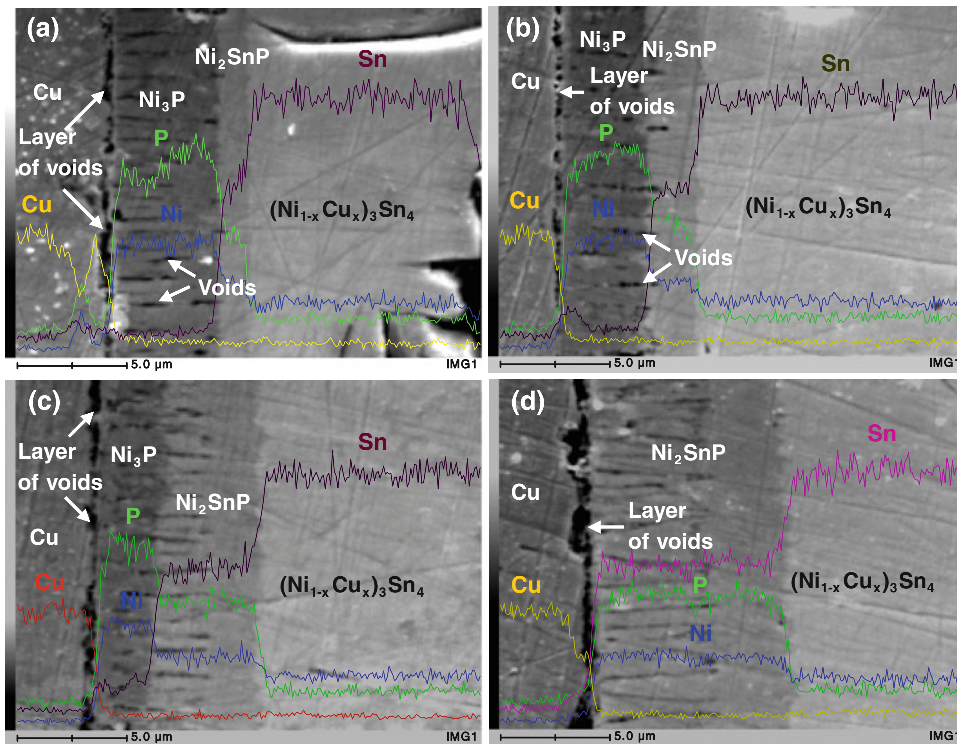

Fig. 4. Line-scan SEM images of the Cu/electroless Ni-P/Sn-3.5Ag interfaces in the samples aged at 200°C for (a) 48 h, (b) 100 h, (c) 225 h, and (d) 400 h, showing the growth of the Ni_2SnP layer at the expense of the Ni_3P layer.

the Ni_3P layer. Concurrently, a layer of voids formed at the Cu/Ni_3P interface. The presence of this layer of voids and the appearance of Cu in Ni_3Sn_4 imply that, after the complete transformation of electroless Ni-P layer into Ni_3P, diffusion of Cu takes place from the Cu/Ni_3P interface to the

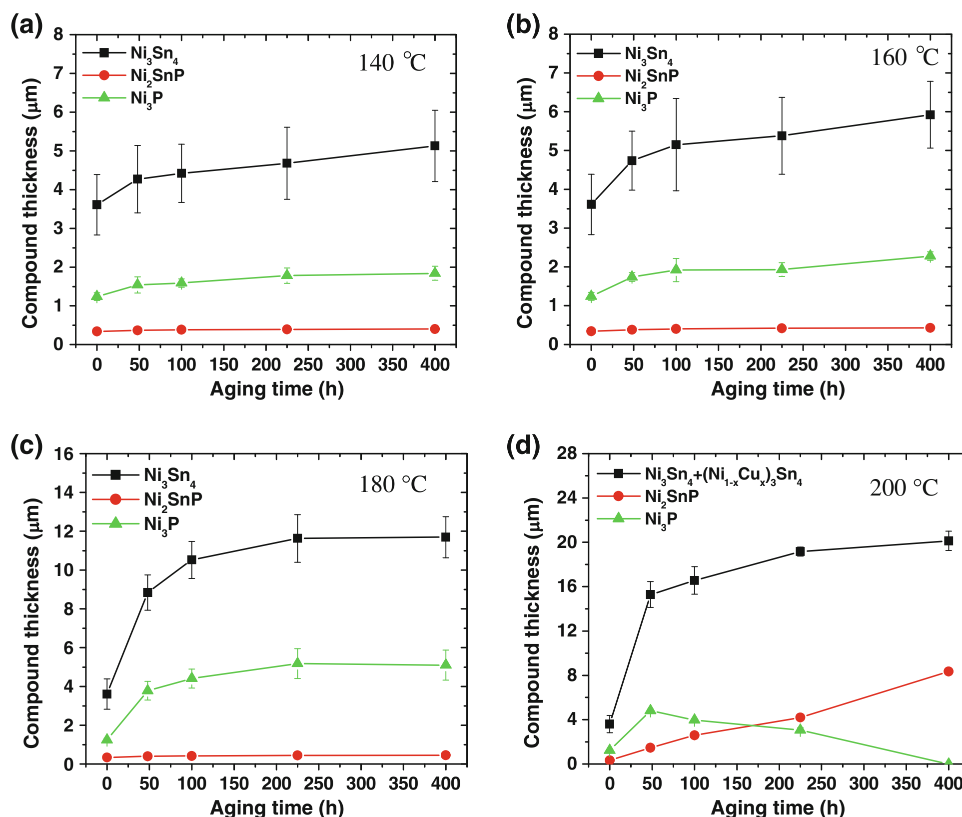

Fig. 5. Thickness of the Ni_3Sn_4, Ni_2SnP, and Ni_3P compounds as a function of aging time at temperatures of (a) 140°C, (b) 160°C, (c) 180°C, and (d) 200°C.

Ni_2SnP/Ni_3Sn_4 interface, resulting in the formation of the layer of voids and $(Ni_{1-x}Cu_x)_3Sn_4$ intermetallics at the Cu/Ni_3P and Ni-Sn-P/Ni_3Sn_4 interfaces, respectively. The extreme case of Cu diffusion in a Cu/Ni-P/Sn-3.5Ag solder joint has been discussed in our previous work,[18] thus it will not be the focus of the current study. Rather, the current work aims to clarify the competing growth mechanism, as well as reporting the related kinetics of the IMCs.

Growth of the IMCs

Figure 5 shows the thickness of the Ni_3Sn_4, Ni_2SnP, and Ni_3P compound layers as a function of aging time at different temperatures. It can be observed that, in the samples aged at 140°C and 160°C, all the layers grew with aging; however, the growth of the Ni_2SnP layer was negligible as compared with the growth of the Ni_3Sn_4 and Ni_3P layers. A similar trend of compound growth was observed in the samples aged at 180°C, however in these samples, compound growth became sluggish at the later stage (after 225 h) of aging. The reason for this sluggish compound growth was the complete transformation of the electroless Ni-P layer into the Ni_3P layer at most of the places along the Sn-3.5Ag/Ni-P/Cu interface (Fig. 2c), which subsequently reduced the supply of Ni from the remaining electroless Ni-P layer. A different trend of compound growth was observed in the samples aged at 200°C, where Ni_3Sn_4 + $(Ni_{1-x}Cu_x)_3Sn_4$ and the Ni_2SnP layers grew and the Ni_3P layer diminished with aging (Fig. 5d). In these samples, the electroless Ni-P layer completely transformed into the Ni_3P layer within 48 h of aging and then the Ni_2SnP layer started to grow rapidly at the expense of the Ni_3P layer.

It has been reported[1,21] that the Ni_3Sn_4 and Ni_3P compounds grown at the electroless Ni-P/solder (Sn-Pb and Sn-Ag) interface are the reaction products of a mass-conservative reaction between Sn and electroless Ni-P and have a constant relation between their thicknesses. In this investigation, we also observed a constant relation between the thicknesses of the Ni_3Sn_4 and Ni_3P layers. Table I shows the layer thickness ratio of Ni_3Sn_4 to Ni_3P measured at different aging conditions. It can be seen that, except for the samples aged at 200°C, the thickness ratio of Ni_3Sn_4 to Ni_3P is within the narrow range of 2.2 to 2.9. The higher thickness ratio in the case of samples aged at 200°C is understood to be caused by the diminishing Ni_3P layer.

Growth Kinetics of the Intermetallic Compounds

Kinetic parameters of IMC growth can be obtained to understand the growth-controlling

Table I. Thickness ratio of the Ni_3Sn_4 to Ni_3P layer measured at different aging conditions

Aging Condition	Thickness Ratio of Ni_3Sn_4 to Ni_3P Layer			
Time (h)/Temperature (°C)	140	160	180	200
0 (as-prepared)	2.9	2.9	2.9	2.9
48	2.8	2.7	2.3	3.2
100	2.8	2.7	2.4	4.2
225	2.6	2.8	2.2	6.3
400	2.8	2.6	2.3	NA

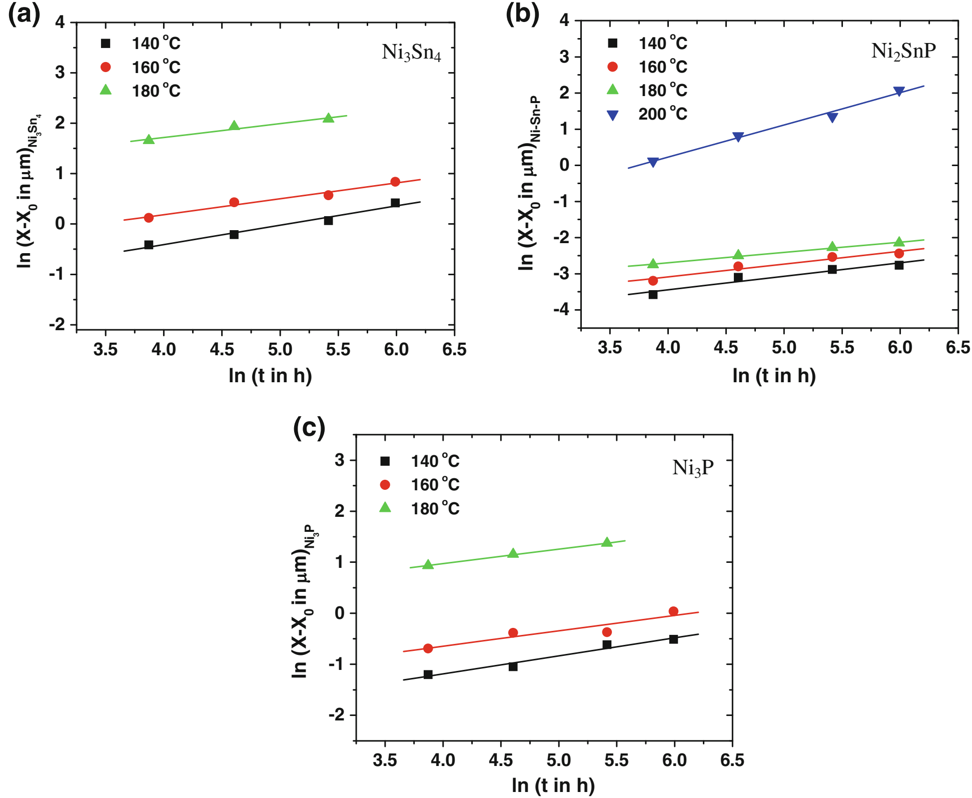

Fig. 6. ln–ln plot of increment in compound thickness versus aging time at various temperatures for (a) Ni_3Sn_4, (b) Ni_2SnP, and (c) Ni_3P.

mechanism. The growth of a compound layer can be represented by the following empirical power law:

$$X = X_0 + kt^{1/n}, \quad (1)$$

where X is the thickness of the compound layer at time t, X_0 is the initial thickness, n is the time exponent, and k is the temperature-dependent rate constant. The variation in k with temperature can be represented by the following Arrhenius equation:

$$k = A\exp(-Q/RT), \quad (2)$$

where A is a prefactor, T is absolute temperature, R is the gas constant, and Q is the apparent activation energy of compound growth. The growth of the compound is controlled by various mechanisms, such as diffusion of reacting elements and the rate of reaction, and this can be predicted by the value of n in Eq. 1. If n is 1, the compound growth is controlled by the rate of reaction, and if n is 2, then the diffusion of the reacting element is the growth-controlling mechanism. However, these are ideal values. In practice, n may deviate from these ideal values due to several factors, such as the formation of multiple compound layers, different diffusion mechanism, and time-dependent apparent diffusivity. Moreover, n can be close to 3 if the growth of the compound takes place in conjunction with grain coarsening of the compound.[23,24]

As shown in Fig. 6, based on Eq. 1, the thickness data of the IMCs were plotted as $\ln(X - X_0)$ (μm) versus $\ln(t)$ (h) to determine the kinetic parameters k and n. The values of $1/n$ and $\ln(k)$ (μm/h$^{1/n}$), respectively, are represented by the slope and the y-axis intercept of the best-fit line to the thickness data. The measured kinetic parameters for the

Table II. Kinetic parameters of the growth of the Ni_3Sn_4, Ni_2SnP, and Ni_3P compounds at various temperatures

Temperature (°C)	Ni_3Sn_4			Ni_2SnP			Ni_3P		
	ln(*k*) (μm/h$^{1/n}$)	1/*n*	*n*	ln(*k*) (μm/h$^{1/n}$)	1/*n*	*n*	ln(*k*) (μm/h$^{1/n}$)	1/*n*	*n*
140	−1.94	0.38	2.63	−4.93	0.37	2.70	−2.60	0.35	2.86
160	−1.08	0.32	3.13	−4.50	0.35	2.86	−1.85	0.30	3.33
180	0.62	0.28	3.57	−3.84	0.29	3.45	−0.16	0.28	3.57
200	NA	NA	NA	−3.34	0.89	1.12	NA	NA	NA

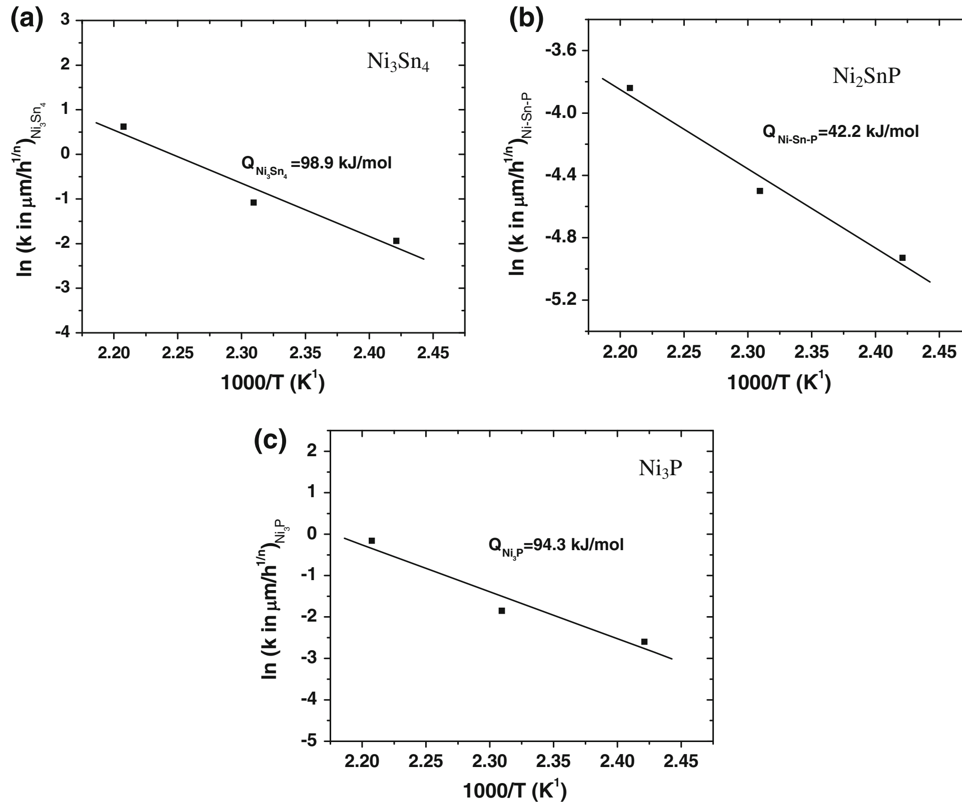

Fig. 7. Arrhenius plot of the (a) Ni_3Sn_4, (b) Ni_2SnP, and (c) Ni_3P growth used to estimate apparent activation energy.

growth of the Ni_3Sn_4, Ni_2SnP, and Ni_3P layers at different temperatures are presented in Table II. The kinetic parameters for Ni_3Sn_4 and Ni_3P growth at 200°C could not be obtained because of the presence of Cu in Ni_3Sn_4 and a decrease in Ni_3P thickness. For the growth of Ni_3Sn_4 and Ni_3P at 180°C, kinetic parameters were obtained by only considering the compound growth up to 225 h of aging. After 225 h, the electroless Ni-P layer was completely transformed into the Ni_3P layer at most of the places along the Sn-3.5Ag/Ni-P interfaces (Fig. 2c). From Table II, the value of n is close to 3. Our preliminary work indicates that compound growth in the Ni-P/Sn-3.5Ag system is controlled by the diffusion of reacting elements through the Ni_3P layer. A similar kinetic result for the growth of Ni_3Sn_4 IMC in the electroless Ni-P/Sn-3.5Ag solder joint has been reported in previous studies.[13,15,22] The value of n obtained from the Ni_2SnP layer implies that its growth was diffusion controlled in the samples aged at 140°C, 160°C, and 180°C but became reaction controlled in the samples aged at 200°C. In the present work, the deviation of the n value from 3 and 1 could be due to the formation of multiple compound layers and time-dependent apparent diffusivity.

Based on Eq. 2, the Arrhenius plots shown in Fig. 7 were obtained for different compounds to estimate the apparent activation energy for compound growth. The activation energies for Ni_3Sn_4, Ni_2SnP, and Ni_3P growth were estimated to be 98.9 kJ/mol, 42.2 kJ/mol, and 94.3 kJ/mol, and the prefactors were 4.1×10^{11} μm/h$^{1/n}$, 1.5×10^{3} μm/h$^{1/n}$, and 5.2×10^{10} μm/h$^{1/n}$ ($n \approx 3$), respectively. The

Table III. Activation energies (*Q*) of the growth of compounds in the electroless Ni-P/solder systems reported in different studies

Solder (wt.%)	Experimental Conditions (Temperature/Time)	Compound	*Q* (kJ/mol)	Reference
Sn-3.5Ag	140–180°C/up to 400 h	Ni_3Sn_4	98.9	Present work
Sn-3.5Ag	140–180°C/up to 400 h	Ni_2SnP	42.2	Present work
Sn-3.5Ag	140–180°C/up to 400 h	Ni_3P	94.3	Present work
Sn-37Pb	200–240°C/up to 40 min	Ni_3P	31.8	1
Sn-3.5Ag	130–170°C/up to 625 h	Ni_3Sn_4	110	12
Sn-37Pb	130–170°C/up to 625 h	Ni_3Sn_4	141	12
Sn-3.5Ag	100–170°C/up to 60 days	Ni_3Sn_4	49	15
Sn-3.5Ag	240–270°C/up to 120 min	Ni_3P	75	21
Sn-3.5Ag-0.5Cu	240–270°C/up to 120 min	Ni_3P	103	21
Sn-0.7Cu	240–270°C/up to 120 min	Ni_3P	131	21

activation energies for Ni_3Sn_4 and Ni_3P growth are very close to each other, which is expected due to the constant relation between their growths (Table I). However, interestingly, despite the slow Ni_2SnP growth, its activation energy (42.2 kJ/mol) is lower than that of Ni_3Sn_4 and Ni_3P growth. Although low activation energy indicates that the barrier to compound growth can be easily overcome, one also has to consider the contribution of the prefactor; in the case of Ni_2SnP, the value of the prefactor was found to be much lower that that of Ni_3Sn_4 and Ni_3P. Table III lists the activation energies of the growth of compounds in electroless Ni-P/solder systems reported in different studies. Considering the fact that the activation energy of compound growth varies widely depending upon solder composition and experimental conditions, our results for the compounds Ni_3Sn_4 and Ni_3P are in agreement with previously reported results.[1,12,15,21] However, for the ternary Ni_2SnP compound, no comparison could be made, as this is the first study to report its growth kinetics. The low activation energy of Ni_2SnP also means that its growth is less dependent on temperature, i.e., increasing reaction temperature will have the least effect on its thickness increase. This probably explains why there have not been any reports on its growth kinetics so far. On the other hand, once the Ni-P metallization is fully consumed, its growth will be very fast, as demonstrated by the current work, following a new controlling mechanism.

DISCUSSION

In this work, it was confirmed that three types of compounds, namely Ni_3Sn_4, Ni_2SnP, and Ni_3P, form during electroless Ni-P/Sn-3.5Ag interfacial reactions. This is in good agreement with some previous studies.[1,6,7,9–11,17,18] Nonetheless, understanding of their growth mechanism remains incomplete. It is known that, during the solder reactions, Sn from the solder reacts with Ni from the electroless Ni-P and forms the Ni_3Sn_4 IMC.[1,2,4] Depletion of Ni from the electroless Ni-P layer results in its transformation into a higher-P-containing Ni-P (Ni_3P) layer.[1,7,18] For further growth of Ni_3Sn_4, Sn diffuses from the solder through the Ni_3Sn_4 layer and Ni diffuses from the electroless Ni-P layer through the Ni_3P layer.[1,4,7,18] At the same time, Sn also reacts with the Ni_3P layer to form a thin layer of Ni_2SnP compound in between the Ni_3Sn_4 and Ni_3P layers. The growth of Ni_2SnP compounds remains slow as long as Ni is available from the electroless Ni-P layer. Once the electroless Ni-P layer is completely transformed into Ni_3P and there is no free Ni to react with Sn, the Ni_2SnP layer starts to grow rapidly, consuming the already formed Ni_3P layer. This unique reaction mechanism results in the formation of the columnar voids in the Ni_3P layer, as there is no compensation for lattice vacancies left by outdiffused Ni. The size and number of these voids increased with increasing Ni_3P thickness during aging (Fig. 2). This implies that the voids in the Ni_3P layer form in conjunction with the transformation of the electroless Ni-P layer into the Ni_3P layer. During this transformation, as shown in Fig. 8, P remains in the Ni-P layer. However, Ni diffuses out from the Ni-P layer, which causes a reduction in the thickness of the Ni-P layer (Fig. 2c). There is no detection of Sn in the Ni_3P layer: it terminates at the interface between the Ni-Sn-P and Ni_3P layers (Fig. 9) due to the reaction with Ni_3P.

Accordingly, the growth mechanism of compounds formed at the Sn-3.5Ag/Ni-P reaction couple can be understood as depicted in Fig. 10. There are mainly three reactions taking place during the electroless Ni-P/solder interfacial reactions: the reaction between Sn and Ni to form Ni_3Sn_4, the transformation of electroless Ni-P into Ni_3P, and the reaction between Sn and Ni_3P to form the Ni_2SnP compound. For these reactions, Sn diffuses from the solder and first reaches the Ni_3Sn_4/Ni_2SnP interface, where it reacts with Ni and forms Ni_3Sn_4. Sn reaches the Ni_2SnP/Ni_3P interface and forms the Ni_2SnP compound by reacting with Ni_3P. At the beginning of the interfacial reactions, growth of the Ni_3Sn_4 and Ni_3P layers is dominant, as most of the Sn coming from the solder is consumed by Ni

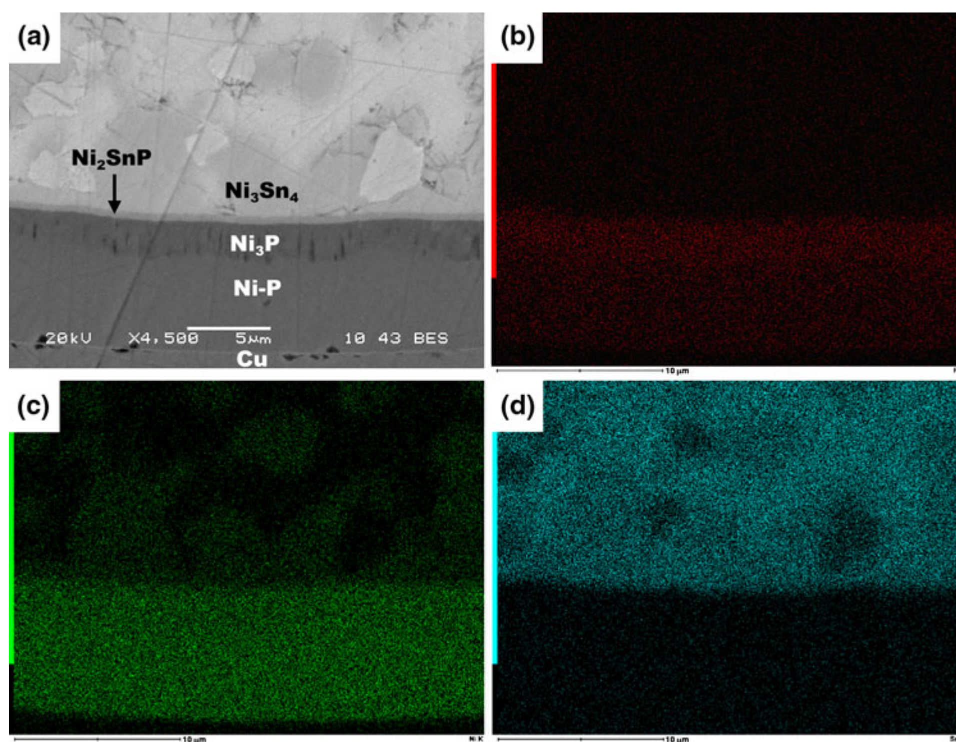

Fig. 8. EDS element mapping analysis of the Sn-3.5Ag/Ni-P/Cu interfaces of the sample aged at 160°C for 400 h: (a) SEM image, (b) mapping for P, (c) mapping for Ni, and (d) mapping for Sn. Elemental concentration decreases with increasing black intensity.

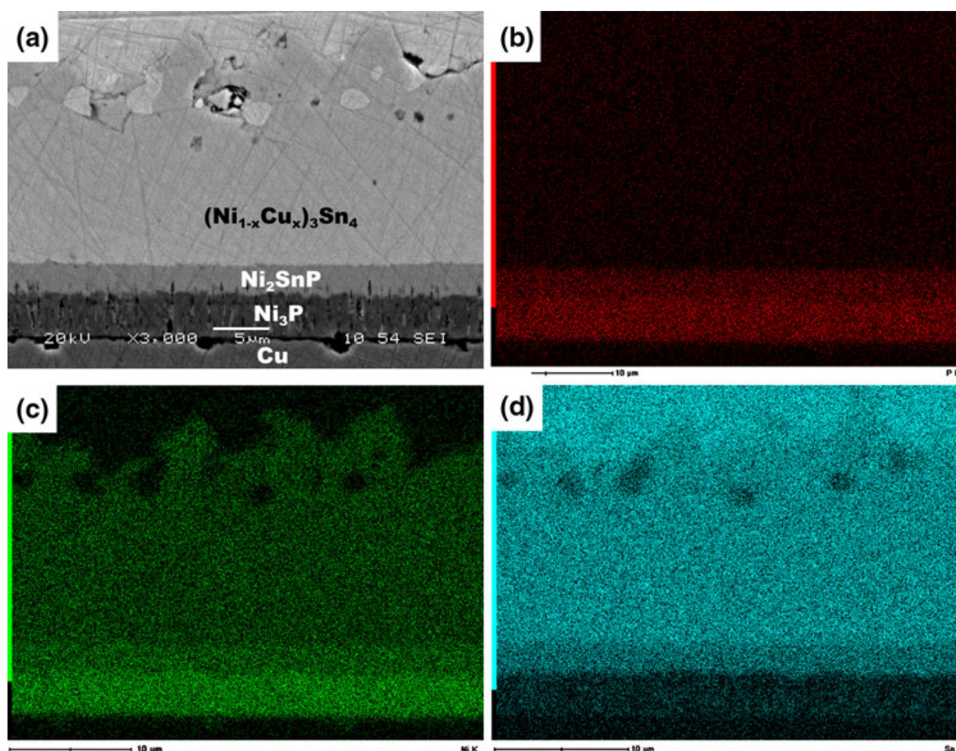

Fig. 9. EDS element mapping analysis of the Sn-3.5Ag/Ni-P/Cu interfaces of the sample aged at 200°C for 100 h: (a) SEM image, (b) mapping for P, (c) mapping for Ni, (d) mapping for Sn. Elemental concentration decreases with increasing black intensity.

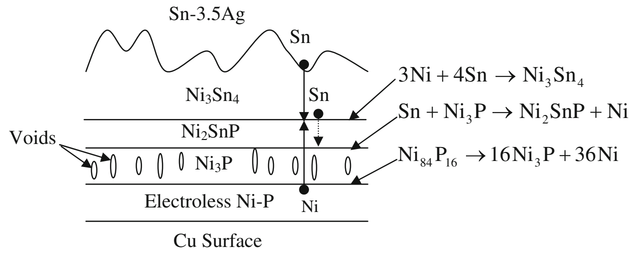

Fig. 10. Schematic illustration of the growth of multiple compounds at the Sn-3.5Ag/electroless Ni-P/Cu interfaces showing all the interfacial reactions.

at the Ni_3Sn_4/Ni_2SnP interface and only a small part of the Sn reaches the Ni_2SnP/Ni_3P interface to react with Ni_3P. However, once the supply of Ni stops as a result of complete transformation of the Ni-P into Ni_3P, the Ni_2SnP compound grows rapidly because Sn now only reacts with Ni_3P according to

$$Sn + Ni_3P \rightarrow Ni_2SnP + Ni \quad (3)$$

To ascertain the reaction between Sn and Ni_3P, the law of conservation of mass was applied to the growth of compound layers in the samples aged at 200°C. In these samples, the electroless Ni-P layer completely transformed into a Ni_3P layer within 48 h of aging, and then the Ni_3P layer completely transformed into a Ni_2SnP layer within 400 h of aging. Thus, according to Eq. 3, if the Ni_3P layer is transformed into the Ni_2SnP layer due to its reaction with Sn, then the number of moles of Ni in the Ni_3P layer present after 48 h of aging must be equal to the total number of moles of Ni in the Ni_2SnP layer and the number of moles of free Ni after 48 h of aging. Since free Ni is consumed in order to grow the Ni_3Sn_4 IMC, the number of moles of free Ni must be equal to the number of moles of Ni in the Ni_3Sn_4 layer grown after 48 h of aging. To simplify the mass balance calculation, the small amount of Cu in $(Ni_{1-x}Cu_x)_3Sn_4$ ($0 \le x \le 0.12$) intermetallics is neglected and the Ni_3Sn_4 + $(Ni_{1-x}Cu_x)_3Sn_4$ layer is assumed to be Ni_3Sn_4 only.

From Fig. 5d, the thickness of the Ni_3P layer at 48 h of aging was 4.8 μm and the growth in the Ni_2SnP and Ni_3Sn_4 layers from 48 h to 400 h of aging was 6.9 μm and 4.8 μm, respectively. The number of moles of Ni in a compound layer of thickness t_{Comp} per unit interfacial area can be determined by

$$Ni_{Comp} = m \times \frac{t_{Comp} d_{Comp}}{M_{Comp}}, \quad (4)$$

where m is the number of moles of Ni in one mole of compound, M_{Comp} is the molecular weight, and d_{Comp} is the compound density. Thus, by inserting the values of m (3 for Ni_3P, 2 for Ni_2SnP, and 3 for Ni_3Sn_4), densities ($d_{Ni_3P} = 7.82$ g/cm^3,[1] $d_{Ni_2SnP} = 7.56$ g/cm^3,[25] and $d_{Ni_3Sn_4} = 8.64$ g/cm^3[1]), molecular weights, and layer thicknesses into Eq. 4, Ni_{Ni_3P}, Ni_{Ni_2SnP}, and $Ni_{Ni_3Sn_4}$ are determined to be 0.54 mol/cm^2, 0.39 mol/cm^2, and 0.19 mol/cm^2. From these values it is clear that $Ni_{Ni_3P} \approx Ni_{Ni_2SnP} + Ni_{Ni_3Sn_4}$. Thus, it is proved that Sn reacts with Ni_3P and Ni (in the Ni-P alloy) to form Ni_2SnP and Ni_3Sn_4 compounds. The slightly higher value of $Ni_{Ni_2SnP} + Ni_{Ni_3Sn_4}$ than that of Ni_{Ni_3P} can be understood by the presence of a small amount of Cu in $(Ni_{1-x}Cu_x)_3Sn_4$ intermetallics, which we neglected in the mass balance calculation.

Based on the kinetics data, the Ni_2SnP layer growth is diffusion controlled initially, but changes to reaction controlled after extensive reaction as in the case of samples aged at 200°C. As the excessive growth of the Ni_2SnP layer can influence the mechanical reliability of electroless Ni-P/solder joints, it is necessary to understand the transition in the Ni_2SnP growth kinetics. In a Ni/Sn reaction couple, Sn is the dominant diffusing element in Ni_3Sn_4.[4] Therefore, the limiting step is Ni diffusion from the electroless Ni-P layer through the Ni_3P and Ni_2SnP layers to meet Sn.[1,7,10,11] Our experimental observations at different temperatures and aging durations confirm our proposed reaction mechanisms. In the samples aged at 140°C, 160°C, and 180°C, where sufficient Ni was available from electroless Ni-P, most of the Sn coming from the solder was consumed by Ni to form Ni_3Sn_4, and therefore the growth of the Ni_2SnP layer was slow. However in the samples aged at 200°C, owing to the complete transformation of the Ni-P layer into Ni_3P, rapid growth of the Ni_2SnP layer occurred. Hence, it can be said that, as long as the electroless Ni-P layer is present underneath the Ni_3P layer, the growth of the Ni_2SnP is slow and is diffusion controlled. Once the Ni-P is fully reacted away, growth of the Ni_2SnP is fast and controlled by the rate of reaction between Sn and Ni_3P. The growth of the ternary Ni_2SnP compound can be suppressed by ensuring a continuous supply of Ni from the electroless Ni-P layer, which can be realized by either increasing the thickness or decreasing the P content of the electroless Ni-P layer. The former is far more effective and practically easier to achieve. As complete consumption of the Ni-P metallization degrades the solder joint severely,[18] thicker Ni-P metallization combined with lower P content could be a solution for enhanced joint reliability.

CONCLUSIONS

Interfacial reactions between Sn-3.5Ag solder and electroless Ni-P metallization were investigated after reflow and high-temperature solid-state aging. Interdependent IMC growth has been observed. The mechanisms were explained and the kinetic data calculated. The following conclusions can be reached based on the investigation:

1. During interfacial reactions, mainly three compounds, Ni_3Sn_4, Ni_2SnP, and Ni_3P, formed at the interface as a result of reaction between Sn and Ni, reaction between Sn and Ni_3P, and self-crystallization of amorphous Ni-P, respectively.

Depletion of Ni from the electroless Ni-P layer resulted in the formation of columnar voids in the Ni_3P layer.
2. Ni_3Sn_4 and Ni_3P layers grow predominantly as long as the electroless Ni-P layer is present at the reaction interface. However, after the complete transformation of the electroless Ni-P layer into Ni_3P, the Ni_2SnP layer grows rapidly at the expanse of the Ni_3P layer.
3. The growth of the Ni_3Sn_4 and Ni_3P layers follows $t^{1/3}$ kinetics. Initially, the growth of the ternary Ni_2SnP compound also follows $t^{1/3}$ kinetics, but after the complete transformation of the electroless Ni-P layer into Ni_3P, it follows linear (t^1) kinetics due to the dominating reaction between Sn with Ni_3P.
4. The apparent activation energies for the growth of Ni_3Sn_4, Ni_2SnP, and Ni_3P compounds are found to be 98.9 kJ/mol, 42.2 kJ/mol, and 94.3 kJ/mol, respectively.

ACKNOWLEDGEMENTS

This work was financially supported by Research Grants RG 14/03 and RG 19/00 to the Nanyang Technological University by the Ministry of Education, Singapore. Technical discussion with Prof. Andriy Gusak, Prof. Joo Tien Oh, and Prof. King Ning Tu is gratefully acknowledged.

REFERENCES

1. J.W. Jang, P.G. Kim, K.N. Tu, D.R. Frear, and P. Thompson, *J. Appl. Phys.* 85, 8456 (1999).
2. J.W. Jang, D.R. Frear, T.Y. Lee, and K.N. Tu, *J. Appl. Phys.* 88, 6359 (2000).
3. G.O. Mallory and J.B. Hajdu, *Electroless Plating: Fundamental and Applications* (Orlando, FL: American Electroplaters and Surface Finishers Society, 1990), pp. 111–113.
4. C.Y. Lee and K.L. Lin, *Thin Solid Films* 249, 201 (1994).
5. M. He, Z. Chen, G.J. Qi, C.C. Wong, and S.G. Mhaisalkar, *Thin Solid Films* 462, 363 (2004).
6. K. Zeng and K.N. Tu, *Mater. Sci. Eng. R* 38, 55 (2002).
7. H. Matsuki, H. Ibuka, and H. Saka, *Sci. Technol. Adv. Mater.* 3, 261 (2002).
8. C.W. Hwang, K. Suganuma, M. Kiso, and S. Hashimoto, *J. Mater. Res.* 18, 2540 (2003).
9. S.J. Wang and C.Y. Liu, *Scripta Mater.* 49, 813 (2003).
10. Z. Chen, M. He, and G.J. Qi, *J. Electron. Mater.* 33, 1465 (2004).
11. M. He, Z. Chen, and G.J. Qi, *Acta Mater.* 52, 2047 (2004).
12. M. He, A. Kumar, P.T. Yeo, G.J. Qi, and Z. Chen, *Thin Solid Films* 462, 387 (2004).
13. M. He, W.H. Lau, G.J. Qi, and Z. Chen, *Thin Solid Films* 462, 376 (2004).
14. Y.C. Sohn, J. Yu, S.K. Kang, D.Y. Shih, and T.Y. Lee, *J. Mater. Res.* 19, 2428 (2004).
15. J.W. Yoon and S.B. Jung, *J. Alloys Compd.* 376, 105 (2004).
16. M. He, Z. Chen, and G.J. Qi, *Metall. Mater. Trans. A* 36, 65 (2005).
17. J.W. Yoon and S.B. Jung, *J. Alloys Compd.* 396, 122 (2005).
18. A. Kumar, Z. Chen, S. Mhaisalkar, C.C. Wong, P.S. Teo, and V. Kripesh, *Thin Solid Films* 504, 410 (2006).
19. Z. Chen, M. He, A. Kumar, and G.J. Qi, *J. Electron. Mater.* 36, 17 (2007).
20. A. Kumar and Z. Chen, *Mater. Sci. Eng. A* 423, 175 (2006).
21. A. Sharif, Y.C. Chan, M.N. Islam, and M.J. Rizvi, *J. Alloys Compd.* 388, 75 (2005).
22. Y.D. Jeon, A. Ostmann, H. Reichl, and K.W. Paik, *Proceedings of the IEEE Electronic Components and Technology Conference* (New Orleans: IEEE, 2003), pp. 1203–1208.
23. G. Ghosh, *Acta Mater.* 48, 3719 (2000).
24. A.M. Gusak and K.N. Tu, *Phys. Rev. B* 66, Article Number 115403 (2000).
25. S. Furuseth and H. Fjellvag, *Acta Chemica Scandinavica A* 39, 537 (1985).